NASA Technical Paper 2868

1989

Mixed Finite Element Models for Free Vibrations of Thin-Walled Beams

Ahmed K. Noor,
Jeanne M. Peters,
and Byung-Jin Min
The George Washington University
Joint Institute for Advancement of Flight Sciences
Langley Research Center
Hampton, Virginia

National Aeronautics and Space Administration
Office of Management
Scientific and Technical Information Division

1989

Contents

Summary 1

Introduction 1

Symbols 1

Mathematical Formulation 2

Comments on Perturbed Lagrangian Formulation 3

Numerical Studies 3

- Cantilever Beams With Channel Cross Sections 4
- Semicircular Beams With Z-Sections 4

Concluding Remarks 5

Acknowledgment 5

Appendix A—Fundamental Equations of Thin-Walled Beam Theory Used in Present Study . . . 6

- Displacement Assumptions 6
- Strain Assumptions 6
- Constitutive Relations 7
- Variational Functional 7

Appendix B—Formulas for Coefficients in Governing Equations for Individual Elements 9

References 10

Tables 11

Figures 12

Summary

Simple, mixed finite element models are developed for the free-vibration analysis of curved, thin-walled beams with arbitrary open cross section. The analytical formulation is based on a linear, Vlasov-type, thin-walled beam theory with the effects of flexural-torsional coupling, transverse shear deformation, and rotary inertia included. The fundamental unknowns consist of seven internal forces and seven generalized displacements of the beam. The element characteristic arrays are obtained by using a modified form of the Hellinger-Reissner mixed variational principle. The modification consists of augmenting the functional of that principle by two terms: (1) the Lagrange multiplier associated with the constant condition relating the rotation of the cross section and the twist degrees of freedom, and (2) a regularization term that is quadratic in the Lagrange multiplier. Only C^0 continuity is required for the generalized displacements. The internal forces and the Lagrange multiplier are allowed to be discontinuous at interelement boundaries.

Numerical results are presented to demonstrate the high accuracy and effectiveness of the elements developed. The standard of comparison is taken to be the solutions obtained by using two-dimensional plate/shell models for the beams.

Introduction

Since the development of the comprehensive theory of combined torsion and bending of thin-walled beams by Vlasov in the 1930's (see Vlasov 1961), extensive literature has been devoted to the application and adaptation of the theory to a variety of equilibrium, stability, and vibration problems of thin-walled structures. Reviews of the many contributions on this subject are given in a number of survey papers (see, for example, Nowinski 1966 and Panovko and Beilin 1969) and monographs (Gjelsvik 1981; Kollbrunner and Basler 1969; Vlasov 1961; and Zbirohowski-Kościa 1967). Several finite element models, based on Vlasov's theory, have been proposed in the literature for the equilibrium, stability, and vibration analysis of thin-walled beams. (See Attard 1986; Barsoum and Gallagher 1970; Epstein and Murray 1976; Friberg 1985; Kiss 1986; Krajcinovic 1969; Mei 1970; Rozmarynowski and Szymczak 1984; Tralli 1986; and Wekezer 1987.) Also, a number of commercial programs have thin-walled beam models in their element libraries. (See, for example, Kiss 1986.) However, except for the hybrid model and the modified displacement model described in Kiss (1986) and Tralli (1986), all the other finite element models developed are based on a standard displacement formulation that requires C^1 continuity for the torsional degrees of freedom. Despite the documented advantages of mixed formulations in finite element modeling, to date no publications exist in which mixed finite elements are used for modeling thin-walled beams. The present study attempts to fill this void. Specifically, the objectives of this paper are: (1) to present simple and efficient mixed finite element models for the free-vibration analysis of curved thin-walled beams with arbitrary open cross section, and (2) to demonstrate the effectiveness of these elements by means of a numerical comparison with results of two-dimensional models.

To sharpen the focus of the study, only prismatic thin-walled beams with open cross section are considered. The wall thickness is assumed to be constant, and the material is linearly elastic and isotropic. The analysis can be extended to anisotropic beams with variable geometric and material characteristics.

Symbols

A	cross-sectional area
A_y, A_z	effective shear areas in y- and z-directions, respectively
B_ω	bimoment
b	flange (or web) dimension
E	Young's modulus
$[F]$	linear flexibility matrix for an individual element
G	shear modulus
$\{H\}$	vector of internal force parameters
I_y, I_z, I_{yz}	second moments of cross section (moments and product of inertia)
$I_\omega, I_{\omega y}, I_{\omega z}$	second sectorial moments of cross section
J	Saint-Venant torsion constant of cross section
K	kinetic energy
L	beam length
l	length of individual finite element
$[M]$	consistent mass matrix for individual element
M_y, M_z, M_t	bending and twisting moments
m	number of displacement nodes in element

N	shape functions used for approximating generalized displacements
$\overline{N}$	shape functions used for approximating internal forces and Lagrange multiplier
N_x	axial force
$[P], [Q]$	elemental matrices associated with constraint condition and regularization term in the functional, respectively
Q_y, Q_z	transverse shear forces
R	radius of curvature of centerline of beam
$[S]$	strain-displacement matrix for individual element
S_ω	first sectorial moment of cross section
s	number of parameters used in approximating each of internal forces and Lagrange multiplier within individual elements
t	wall thickness
U	total strain energy
U^c	complementary strain energy
U_n	strain energy associated with normal stresses (N_x, M_y, M_z, and B_ω)
U_{ts}	strain energy associated with torsional shear stresses (M_t)
u, v, w	displacement components in coordinate directions
u^0, v^0, w^0	axial and transverse displacements at $y = z = 0$
$\{X\}$	vector of nodal displacements
x, y, z	orthogonal coordinate system with x passing through centroids of cross sections
γ_{xy}, γ_{xz}, $\gamma^0_{xy}, \gamma^0_{xz}$	transverse shear strains (see eqs. (A2), appendix A)
ε	penalty parameter
ε_x	extensional strain
ε^0_x	extensional strain of centerline of beam
ζ	contour coordinate used in evaluating sectorial coordinate ω
θ^0	rate of twist of beam
$\kappa^0_y, \kappa^0_z, \kappa^0_t$	curvature changes and twist of beam
$\bar{\lambda}$	Lagrange multiplier
$\{\lambda\}$	vector of Lagrange multiplier parameters
ρ	mass density of material
$\sigma_x, \sigma_{xy}, \sigma_{xz}$	normal and shearing stresses on cross section
υ	Poisson's ratio of the material
$\phi^0_x, \phi^0_y, \phi^0_z$	rotation components
ψ^0	strain parameter
Ω	frequency of vibration, Hz
ω	sectorial coordinate (warping of cross section for a unit rate of twist)
∂	$\equiv d/dx$

Range of indices:

i, j	1 to s
i, j	1 to m

Subscripts:

2d	two-dimensional model result
s	shear center

Superscript:

t	matrix transposition

Mathematical Formulation

The analytical formulation is based on a linear form of Vlasov's thin-walled beam theory with the effects of flexural-torsional coupling, transverse shear deformation, and rotary inertia included. A mixed formulation is used in which the fundamental unknowns consist of the seven generalized displacements and seven internal forces. The generalized displacements consist of the axial and transverse displacement components of the centroid u^0, v^0, and w^0; the three rotation components ϕ^0_x, ϕ^0_y, and ϕ^0_z; and the rate of twist of the beam θ^0. The seven internal forces consist of the axial force N_x; the two

transverse shear forces Q_y and Q_z; the two bending moments M_y and M_z; the twisting moment M_t; and the bimoment B_ω. The sign convention for the generalized displacements and internal forces is given in figure 1. The fundamental equations of the thin-walled beam theory used herein are summarized in appendix A. In order to reduce the continuity requirements for all the generalized displacements to C^0, a modified form of the Hellinger-Reissner mixed variational principle (Washizu 1974) is used in the development of the element characteristics. The modification amounts to augmenting the functional of that principle by two terms: the Lagrange multiplier associated with the constraint condition relating ϕ_x^0 and θ^0, and a regularization term that is quadratic in the Lagrange multiplier. (See appendix A.) For a detailed discussion of the augmented (perturbed) Lagrangian formulation, see Fortin and Glowinski (1983).

The shape functions used in approximating the internal forces and the Lagrange multiplier are selected to be the same but are different from those used in approximating the generalized displacements. Moreover, the continuity of both the internal forces and the Lagrange multiplier is not imposed at interelement boundaries.

The finite element equations for each individual element can be cast in the following compact form:

$$\begin{bmatrix} -F & \cdot & S \\ \cdot & \frac{P}{\epsilon} & Q^t \\ S^t & Q & \cdot \end{bmatrix} \begin{Bmatrix} H \\ \lambda \\ X \end{Bmatrix} = \Omega^2 \begin{bmatrix} \cdot & \cdot & \cdot \\ \cdot & \cdot & \cdot \\ \cdot & \cdot & M \end{bmatrix} \begin{Bmatrix} H \\ \lambda \\ X \end{Bmatrix} \quad (1)$$

where $\{H\}$, $\{\lambda\}$, and $\{X\}$ are the internal force parameters, Lagrange multiplier parameters, and nodal displacements, respectively; $[F]$ is the matrix of linear flexibility coefficients; $[S]$ is the strain-displacement matrix; $[P]$ and $[Q]$ are matrices associated with the constraint condition and the regularization term in the functional, respectively (see appendix A); $[M]$ is the consistent mass matrix; Ω is the frequency of vibration; ϵ is a penalty parameter associated with the regularization term; and a dot $(\cdot)$ refers to a zero submatrix. The formulas for the elemental arrays $[F]$, $[S]$, $[P]$, $[Q]$, and $[M]$ are given in appendix B.

If the internal force parameters and the Lagrange multiplier parameters are eliminated from equations (1), one obtains the following equation in the nodal displacements $\{X\}$:

$$\left([S]^t[F]^{-1}[S] - \epsilon[Q][P]^{-1}[Q]^t\right)\{X\} = \Omega^2[M]\{X\} \quad (2)$$

Comments on Perturbed Lagrangian Formulation

The following three comments regarding the perturbed Lagrangian formulation used herein seem to be in order:

1. The governing finite element equations of the perturbed Lagrangian formulation (eqs. (1)) include both those of the Lagrange multiplier approach and the penalty method as special cases as follows:

(1) By letting the penalty parameter ϵ go to infinity, equations (1) reduce to those of the Lagrange multiplier approach.

(2) By eliminating the Lagrange multiplier terms from equations (1), the resulting equations are identical to those of the penalty method.

2. The perturbed Lagrangian formulation, in addition to reducing the continuity requirements for the generalized displacements in the element development, alleviates two of the drawbacks of the Lagrange multiplier approach and the penalty method, namely:

(1) The regularization term in the functional results in replacing one of the zero diagonal blocks in the discrete equations of the Lagrange multiplier approach by the diagonal matrix $[P]/\epsilon$ in equations (1).

(2) The constraint condition relating the rotation of the cross section ϕ_x^0 and the rate of twist θ^0 (see appendix A) is enforced exactly in the functional rather than approximately as in the penalty method. However, the presence of the regularization term results in replacing the constraint condition by the perturbed condition (on the element level):

$$\frac{[P]}{\epsilon}\{\lambda\} + [Q]^t\{X\} = 0 \quad (3)$$

3. An important consideration in the perturbed Lagrangian formulation is the proper selection of the penalty parameter ϵ. With the foregoing mixed models, the penalty parameter can be chosen independently of the element size without adversely affecting the performance of the model. The accuracy of the solution increases with increasing value of the penalty parameter. However, for very large values of ϵ, ill-conditioning of the equations occurs, thereby increasing the round-off errors. In the present study, for convenience, the penalty parameter ϵ was chosen to be equal to the extensional stiffness of the beam EA.

Numerical Studies

To test and evaluate the performance of the foregoing mixed models, a large number of vibration

problems of thin-walled beams with open cross section have been solved by using these models. For each problem, comparison was made with solutions obtained by using two-dimensional plate/shell elements in modeling the beam, and also with previously published solutions whenever available. Herein, the results of two sets of free-vibration problems are discussed. The two problems are: (1) a straight cantilever beam with symmetric and unsymmetric channel cross sections; and (2) a semicircular beam with a Z-shaped section (Z-section) and clamped ends. A classical Rayleigh-Ritz solution along with test results for the first problem are given by Gere and Lin (1958). Also, a finite element solution for the same problem based on displacement models is given by Mei (1970).

In each case, the structure was analyzed using (1) the mixed one-dimensional models developed herein, and (2) two-dimensional plate/shell models based on a Sanders-Budiansky type of shell theory with the effects of transverse shear deformation and rotary inertia included. (See Noor and Andersen 1982 and Noor and Peters 1983 for a description of the finite element model used.) In the one-dimensional models, Lagrangian interpolation functions were used for approximating each of the generalized displacements, internal forces, and Lagrange multiplier. The polynomial functions for the internal forces and the Lagrange multiplier were one degree lower than those of the generalized displacements. The characteristics of the finite element models in the numerical studies are summarized in table I. In all the solutions presented herein, only the displacement boundary conditions are enforced and the force boundary conditions are not applied. Typical results are presented in figures 2 through 7 for the cantilever beams with channel sections and in figures 8 through 12 for the semicircular beams with Z-sections. Also, table II lists the minimum six frequencies obtained by the thin-walled beam and two-dimensional models for the unsymmetric channel section and Z-section.

Cantilever Beams With Channel Cross Sections

The first problem set considered is that of the cantilever beams with the symmetric and the unsymmetric channel cross sections shown in figure 2. The vibration mode shapes for the beam with symmetric channel section, obtained by the two-dimensional model, are shown in figure 3. The ratios of the strain energies associated with normal stresses and torsional shear stresses to the total strain energy, U_n/U and U_{ts}/U, for the first six vibration modes are shown in figure 4. Note that U_n is associated with N_x, M_y, M_z, and B_ω; and U_{ts} is associated with M_t. Except for the second and sixth modes of the beam with symmetric channel section, all the other modes exhibit strong flexural-torsional coupling. This strong coupling cannot be predicted by ordinary beam models in which B_ω is neglected. For all the six modes, the transverse shear strain energy was found to be negligible (less than 0.6 percent of the total energy).

Figures 5 and 6 give an indication of the accuracy and convergence of the first six frequencies obtained by using the M3-2 and M4-3 models. (See table I.) The standard for comparison was taken to be the two-dimensional-model solution obtained using a 20×12 grid of M9-4 elements (20 elements along the beam length). As can be seen from figures 5 and 6, the frequencies predicted by the mixed models were highly accurate and converged rapidly with the increase in the number of elements. Thus, the converged frequencies obtained by the thin-walled beam model were close to those obtained by the two-dimensional model. The maximum error in the lowest six frequencies obtained by the converged thin-walled beam models was less than 1 percent.

The effect of the magnitude of the penalty parameter on the accuracy of the lowest six frequencies obtained by the mixed models is depicted in figure 7. As can be seen, the accuracy of the frequencies obtained by the mixed models is fairly insensitive to the choice of ε in the range of ε/EA from 10^{-3} to 10^{2}. The upper limit of ε is a function of the number of significant digits in the computer.

Semicircular Beams With Z-Sections

The second problem is that of the clamped semicircular beams with the Z-sections of equal and unequal flanges. (See fig. 8.) Henceforth, the equal and unequal flange sections will be referred to as the "symmetric and unsymmetric Z-sections." Because of the spanwise symmetry of the structure, only half the beam was modeled. The vibration mode shapes associated with the lowest six frequencies for the beam with symmetric Z-section are shown in figure 9. These mode shapes are obtained by the two-dimensional model. The ratios of the strain energies U_n/U and U_{ts}/U obtained by the thin-walled beam model for the six vibration modes are shown in figure 10. Again, for all six modes the transverse shear strain energy was found to be less than 0.6 percent of the total energy.

An indication of the accuracy and convergence of the frequencies obtained by the M3-2 and M4-3 models for the beams with symmetric and unsymmetric sections is given in figures 11 and 12. Although the

frequencies predicted by the thin-walled beam models converge rapidly with increasing the number of elements, the errors in the converged frequencies obtained by the thin-walled beam model are greater than those for the straight beam described in the previous subsection. The maximum error in the lowest six frequencies for the beam with unsymmetric Z-section was of the order of 7.5 percent. (See fig. 12 and table II.) The accuracy degradation for the beam with unsymmetric Z-section may be attributed to the cross-sectional distortions that are more pronounced in the mode shapes of the semicircular beam than in those of the straight beam.

Concluding Remarks

Simple, mixed finite element models are developed for the free-vibration analysis of curved, thin-walled beams with arbitrary open cross section. The analytical formulation is based on a linear, Vlasov-type, thin-walled beam theory with the effects of flexural-torsional coupling, transverse shear deformation, and rotary inertia included. The fundamental unknowns consist of seven internal forces and seven generalized displacements of the beam. The element characteristic arrays are obtained by using a modified form of the Hellinger-Reissner mixed variational principle. The modification consists of augmenting the functional of that principle by two terms: (1) the Lagrange multiplier associated with the constraint condition relating the rotation of the cross section and the twist degrees of freedom, and (2) a regularization term that is quadratic in the Lagrange multiplier. Only C^0 continuity is required for the generalized displacements. The internal forces and the Lagrange multiplier are allowed to be discontinuous at interelement boundaries.

The high accuracy and effectiveness of the mixed models developed are demonstrated by means of numerical examples of thin-walled beams with symmetric and unsymmetric cross sections. The standard of comparison in these examples is taken to be the solutions obtained by using two-dimensional plate/shell models for the beams. The accuracy of the mixed models developed is dependent on the cross-sectional distortions during the beam deformations. As the cross-sectional distortions increase, the degradation of accuracy becomes more pronounced.

Acknowledgment

The present research is supported by NASA Grant NAG1-730. The authors appreciate the help of Jeffrey A. Cerro, Planning Research Corporation, Hampton, Virginia, in generating some of the figures, and they acknowledge useful discussions with Huey D. Carden of the NASA Langley Research Center. The numerical results were conducted on the CRAY-2 computer at the NASA Ames Research Center.

NASA Langley Research Center
Hampton, VA 23665-5225
December 15, 1988

Appendix A

Fundamental Equations of Thin-Walled Beam Theory Used in Present Study

The fundamental equations of the linear, Vlasov-type theory of curved thin-walled beams are given in this appendix. A right-handed orthogonal coordinate system is used with the x-axis passing through the centroids of the cross sections. (See fig. 1.) The beam is assumed to be curved in one direction only (in the xz-plane).

Displacement Assumptions

Based on the assumption that the projection of each cross section on a plane normal to the initial centroidal axes does not distort during deformation, the displacement field in the plane of the cross section (yz-plane) is represented by

$$\begin{Bmatrix} u(x,y,z) \\ v(x,y,z) \\ w(x,y,z) \end{Bmatrix} = \begin{Bmatrix} u^0 \\ v^0 \\ w^0 \end{Bmatrix} + \begin{bmatrix} \cdot & z & -y \\ -z & \cdot & \cdot \\ y & \cdot & \cdot \end{bmatrix} \begin{Bmatrix} \phi_x^0 \\ \phi_y^0 \\ \phi_z^0 \end{Bmatrix} - \begin{Bmatrix} \omega \\ \cdot \\ \cdot \end{Bmatrix} \theta^0 \tag{A1}$$

where u^0, v^0, and w^0 are the axial and transverse displacement components at $y = z = 0$; ϕ_x^0, ϕ_y^0, and ϕ_z^0 are the rotation components about the coordinate axes; θ^0 is the rate of twist of the beam; and ω is the sectorial coordinate (warping of the cross section for a unit rate of twist). The seven generalized displacement parameters u^0, v^0, w^0, ϕ_x^0, ϕ_y^0, ϕ_z^0, and θ^0 are functions of x only.

Strain Assumptions

The following expressions are used for the three nonzero components of the strain field in the plane of the cross section:

$$\left.\begin{aligned} \varepsilon_x &= \varepsilon_x^0 - y\kappa_y^0 + z\kappa_z^0 - \omega\psi^0 \\ \gamma_{xy} &= \gamma_{xy}^0 - z\kappa_t^0 \\ \gamma_{xz} &= \gamma_{xz}^0 + y\kappa_t^0 \end{aligned}\right\} \tag{A2}$$

where ε_x^0 is the extensional strain of the centerline; κ_y^0 and κ_z^0 are the curvature changes in the y- and z-directions, respectively; κ_t^0 is the twist; and γ_{xy}^0 and γ_{xz}^0 are the transverse shear strains. The strain parameters ε_x^0, κ_y^0, κ_z^0, γ_{xz}^0, γ_{xy}^0, κ_t^0, and ψ^0 are functions of x only and can be expressed in terms of the displacement and rotation components as follows:

$$\left.\begin{aligned} \varepsilon_x^0 &= \partial u^0 + \frac{w^0}{R} \\ \kappa_y^0 &= \partial\phi_z^0 - \frac{\phi_x^0}{R} \\ \kappa_z^0 &= \partial\phi_y^0 \\ \gamma_{xy}^0 &= \partial v^0 - \phi_z^0 \\ \gamma_{xz}^0 &= -\frac{u^0}{R} + \partial w^0 + \phi_y^0 \\ \kappa_t^0 &= \partial\phi_x^0 + \frac{\phi_z^0}{R} \\ \psi^0 &= \partial\theta^0 \end{aligned}\right\} \tag{A3}$$

where $\partial \equiv d/dx$ and R is the radius of curvature of the centerline of the beam. Also, the following constraint condition is used to relate θ^0 and ϕ_x^0:

$$\partial\phi_x^0 - \theta^0 = 0 \tag{A4}$$

Constitutive Relations

The relations between the internal forces and the strain components are given by

$$\begin{Bmatrix} N_x \\ M_z \\ M_y \\ B_\omega \end{Bmatrix} = \int_A \sigma_x \begin{Bmatrix} 1 \\ -y \\ z \\ \omega \end{Bmatrix} dA = E \begin{bmatrix} A & \cdot & \cdot & -S_\omega \\ & I_z & -I_{yz} & I_{\omega z} \\ & & I_y & -I_{\omega y} \\ \text{Symm} & & & I_\omega \end{bmatrix} \begin{Bmatrix} \varepsilon_x^0 \\ \kappa_y^0 \\ \kappa_z^0 \\ \psi^0 \end{Bmatrix} \tag{A5}$$

and

$$\begin{Bmatrix} Q_y \\ Q_z \\ M_t \end{Bmatrix} = \int_A \begin{bmatrix} 1 & \cdot \\ \cdot & 1 \\ -z & y \end{bmatrix} \begin{Bmatrix} \sigma_{xy} \\ \sigma_{xz} \end{Bmatrix} dA = G \begin{bmatrix} A_y & \cdot & \cdot \\ \cdot & A_z & \cdot \\ \cdot & \cdot & J \end{bmatrix} \begin{Bmatrix} \gamma_{xy}^0 \\ \gamma_{xz}^0 \\ \kappa_t^0 \end{Bmatrix} \tag{A6}$$

where A is the cross-sectional area; S_ω is the first sectorial moment of the cross section; I_y, I_z, and I_{yz} are the second moments of the cross section (moments and product of inertia); J is the Saint-Venant torsion constant; I_ω, $I_{\omega y}$, and $I_{\omega z}$ are the second sectorial moments of the cross section (sectorial moments of inertia); E and G are the Young's and shear moduli of the material, respectively; N_x is the axial force; M_y and M_z are the bending moments; B_ω is the bimoment; Q_y and Q_z are the transverse shearing forces; and M_t is the twisting moment. The definition of the sectorial properties of the cross section is given by Friberg (1985), Heins and Wang (1978), Vlasov (1961), and Zbirohowski-Kościa (1967).

Variational Functional

The functional used in the element development is given by

$$\pi = \pi_{\text{HR}} + \int_0^l \overline{\lambda} \left(\partial \phi_x^0 - \theta^0 \right) dx - \frac{1}{2\varepsilon} \int_0^l (\overline{\lambda})^2 \, dx$$

where $\overline{\lambda}$ is the Lagrange multiplier, ε is a penalty parameter, l is the length of the element, and π_{HR} is the functional of the Hellinger-Reissner mixed variational principle. The expression for π_{HR} is

$$\pi_{\text{HR}} = \int_0^l (V - U^c + K) dx \tag{A7}$$

where

$$V = \begin{Bmatrix} N_x \\ M_z \\ M_y \\ B_\omega \end{Bmatrix}^t \begin{Bmatrix} \varepsilon_x^0 \\ \kappa_y^0 \\ \kappa_z^0 \\ \psi^0 \end{Bmatrix} + \begin{Bmatrix} Q_y \\ Q_z \\ M_t \end{Bmatrix}^t \begin{Bmatrix} \gamma_{xy}^0 \\ \gamma_{xz}^0 \\ \kappa_t^0 \end{Bmatrix} \tag{A8}$$

$$U^c = \frac{1}{2E} \begin{Bmatrix} N_x \\ M_z \\ M_y \\ B_\omega \end{Bmatrix}^t \begin{bmatrix} A & \cdot & \cdot & -S_\omega \\ & I_z & -I_{yz} & I_{\omega z} \\ & & I_y & -I_{\omega y} \\ & \text{Symm} & & I_\omega \end{bmatrix}^{-1} \begin{Bmatrix} N_x \\ M_z \\ M_y \\ B_\omega \end{Bmatrix}$$

$$+ \frac{1}{2G} \begin{Bmatrix} Q_y \\ Q_z \\ M_t \end{Bmatrix}^t \begin{bmatrix} \frac{1}{A_y} & \cdot & \cdot \\ & \frac{1}{A_z} & \cdot \\ \text{Symm} & & \frac{1}{J} \end{bmatrix} \begin{Bmatrix} Q_y \\ Q_z \\ M_t \end{Bmatrix} \tag{A9}$$

$$K = \frac{\rho}{2}\Omega^2 \left\{ A\left[(u^0)^2 + (v^0)^2 + (w^0)^2\right] + (I_y + I_z)\left(\phi_x^0\right)^2 + I_y\left(\phi_y^0\right)^2 + I_z\left(\phi_z^0\right)^2 - 2I_{yz}\phi_y^0\phi_z^0 \right.$$
$$\left. + 2\left(S_\omega u^0 - I_{\omega y}\phi_y^0 + I_{\omega z}\phi_z^0\right)\theta^0 + I_\omega(\theta^0)^2 \right\} \tag{A10}$$

where ρ is the mass density of the material. Note in equations (A5) through (A10) that y and z are centroidal coordinates. (See fig. 1.) The sectorial properties of the cross section are evaluated using the centroid as the pole and the origin of the contour coordinates ς as the lower free end of the cross section. (See fig. 1.) A FORTRAN program for evaluating the sectorial properties is listed by Coyette (1987).

Appendix B

Formulas for Coefficients in Governing Equations for Individual Elements

The explicit forms of the elemental arrays $[F]$, $[S]$, $[P]$, $[Q]$, and $[M]$ are given in this appendix. For convenience, each of these arrays is partitioned into blocks according to contributions from individual nodes, internal forces, or Lagrange multiplier parameters. The expressions of the typical partitions (or blocks) are given in table BI. Note that the order of internal force parameters is N_x, M_z, M_y, B_ω, Q_y, Q_z, and M_t; the order of the generalized displacement coefficients is u^0, v^0, w^0, ϕ_x^0, ϕ_y^0, ϕ_z^0, and θ^0.

In table BI, $\overline{N}^i$ and $\overline{N}^j$ are the shape functions for both the internal forces and the Lagrange multiplier; N^j represents the shape functions for the generalized displacements; R is the radius of curvature; m is the number of displacement nodes in the element; $[I]$ is the identity submatrix; s is the number of parameters used in approximating each of the internal forces and the Lagrange multiplier; l is the length of the element; and $\partial \equiv d/dx$. The range of the indices i and j is 1 to s, and the range of the indices i and j is 1 to m. The dots in the matrices refer to zero terms.

Table BI. Explicit Form of Typical Partitions of the Arrays $[F]$, $[S]$, $[P]$, $[Q]$, and $[M]$

Array	Number of partitions (blocks)	Typical partition (block)
$[F]$	$s \times s$	$\int_0^l \overline{N}^i \overline{N}^j \begin{bmatrix} EA & \cdot & \cdot & -ES_\omega & \cdot & \cdot & \cdot \\ & EI_z & -EI_{yz} & EI_{\omega z} & \cdot & \cdot & \cdot \\ & & EI_y & -EI_{\omega y} & \cdot & \cdot & \cdot \\ & & & EI_\omega & \cdot & \cdot & \cdot \\ & & & & GA_y & \cdot & \cdot \\ & & & & & GA_z & \cdot \\ & & & & & & GJ \end{bmatrix}^{-1} dx$
$[S]$	$s \times \mathrm{m}$	$\int_0^l \overline{N}^i \begin{bmatrix} \partial & \cdot & \frac{1}{R} & \cdot & \cdot & \cdot & \cdot \\ \cdot & \cdot & \cdot & -\frac{1}{R} & \cdot & \partial & \cdot \\ \cdot & \cdot & \cdot & \cdot & \partial & \cdot & \cdot \\ \cdot & \cdot & \cdot & \cdot & \cdot & \cdot & \partial \\ \cdot & \partial & \cdot & \cdot & \cdot & -1 & \cdot \\ -\frac{1}{R} & \cdot & \partial & \cdot & 1 & \cdot & \cdot \\ \cdot & \cdot & \cdot & \partial & \cdot & \frac{1}{R} & \cdot \end{bmatrix} N^j \, dx$
$[P]$	$s \times s$	$\int_0^l \overline{N}^i \overline{N}^j \, dx$
$[Q]$	$s \times \mathrm{m}$	$\int_0^l \overline{N}^i [\ldots \partial \ldots -1] N^j \, dx$
$[M]$	$\mathrm{m} \times \mathrm{m}$	$\int_0^l N^i N^j \rho \begin{bmatrix} A & \cdot & \cdot & \cdot & \cdot & \cdot & -S_\omega \\ & A & \cdot & \cdot & \cdot & \cdot & \cdot \\ & & A & \cdot & \cdot & \cdot & \cdot \\ & & & I_y + I_z & \cdot & \cdot & \cdot \\ & & & & I_y & -I_{yz} & -I_{\omega y} \\ & \text{Symm} & & & & I_z & I_{\omega z} \\ & & & & & & I_\omega \end{bmatrix} dx$

References

Attard, Mario M.: Lateral Buckling Analysis of Beams by the FEM. *Comput. & Struct.*, vol. 23, no. 2, 1986, pp. 217–231.

Barsoum, Roshdy S.; and Gallagher, Richard H.: Finite Element Analysis of Torsional and Torsional-Flexural Stability Problems. *Int. J. Numer. Methods Eng.*, vol. 2, no. 3, July–Sept. 1970, pp. 335–352.

Coyette, J. P.: An Improved Subroutine for the Estimation of Torsional Properties of Thin Walled Open Cross-Sections. *Eng. Comput.*, vol. 4, no. 3, Sept. 1987, pp. 240–242.

Epstein, Marcelo; and Murray, David W.: Three-Dimensional Large Deformation Analysis of Thin Walled Beams. *Int. J. Solids & Struct.*, vol. 12, no. 12, 1976, pp. 867–876.

Fortin, Michel; and Glowinski, Roland: *Augmented Lagrangian Methods: Applications to the Numerical Solution of Boundary-Value Problems.* North-Holland, 1983.

Friberg, P. O.: Beam Element Matrices Derived From Vlasov's Theory of Open Thin-Walled Elastic Beams. *Int. J. Numer. Methods Eng.*, vol. 21, no. 7, July 1985, pp. 1205–1228.

Gere, J. M.; and Lin, Y. K.: Coupled Vibrations of Thin-Walled Beams of Open Cross Section. *J. Appl. Mech.*, vol. 25, no. 3, Sept. 1958, pp. 373–378.

Gjelsvik, Atle: *The Theory of Thin Walled Bars.* John Wiley & Sons, Inc., c.1981.

Heins, C. P.; and Wang, R. C.: Torsional Properties of Open Cross Sections. *Comput. & Struct.*, vol. 9, no. 6, Nov. 1978, pp. 495–500.

Kiss, Ferenc: *The New Family of General Beam Elements for ASKA—Theoretical Manual.* IKO Software Service GmbH (Stuttgart), 1986.

Kollbrunner, C. F.; and Basler, K. (E. C. Glauser, transl., and Annotations and Appendix by B. G. Johnston): *Torsion in Structures—An Engineering Approach.* Springer-Verlag, 1969.

Krajcinovic, Dusan: A Consistent Discrete Elements Technique for Thinwalled Assemblages. *Int. J. Solids & Struct.*, vol. 5, no. 7, July 1969, pp. 639–662.

Mei, Chuh: Coupled Vibrations of Thin-Walled Beams of Open Section Using the Finite Element Method. *Int. J. Mech. Sci.*, vol. 12, no. 10, Oct. 1970, pp. 883–891.

Noor, Ahmed K.; and Andersen, C. M.: Mixed Models and Reduced/Selective Integration Displacement Models for Nonlinear Shell Analysis. *Int. J. Numer. Methods Eng.*, vol. 18, no. 10, Oct. 1982, pp. 1429–1454.

Noor, Ahmed K.; and Peters, Jeanne M.: Mixed Models and Reduced Selective Integration Displacement Models for Vibration Analysis of Shells. *Hybrid and Mixed Finite Element Methods,* S. N. Atluri, R. H. Gallagher, and O. C. Zienkiewicz, eds., John Wiley & Sons Ltd., c.1983, pp. 537–564.

Nowinski, J. L.: Theory of Thin-Walled Bars. *Applied Mechanics Surveys,* H. Norman Abramson, Harold Liebowitz, John M. Crowley, and Stephen Juhasz, eds., Spartan Books, 1966, pp. 325–338.

Panovko, Ya. G.; and Beilin, E. A.: Thin-Walled Beams and Systems Consisting of Thin-Walled Beams. *Structural Mechanics in the USSR—1917–1967,* I. M. Rabinovich, ed., Moscow Publ. House, 1969, pp. 75–98. (In Russian.)

Rozmarynowski, B.; and Szymczak, C.: Non-Linear Free Torsional Vibrations of Thin-Walled Beams With Bisymmetric Cross-Section. *J. Sound & Vibration,* vol. 97, no. 1, Nov. 8, 1984, pp. 145–152.

Tralli, A.: A Simple Hybrid Model for Torsion and Flexure of Thin-Walled Beams. *Comput. & Struct.*, vol. 22, no. 4, 1986, pp. 649–658.

Vlasov, V. Z. (Y. Schechtman, transl.): *Thin-Walled Elastic Beams.* Israel Program for Scientific Translations, 1961.

Washizu, Kyuichiro: *Variational Methods in Elasticity and Plasticity,* Second ed. Pergamon Press Inc., c.1974.

Wekezer, Jerzy W.: Free Vibrations of Thin-Walled Bars With Open Cross Sections. *J. Eng. Mech.*, vol. 113, no. 10, Oct. 1987, pp. 1441–1453.

Zbirohowski-Kościa, K.: *Thin Walled Beams—From Theory to Practice.* Crosby Lockwood & Son Ltd., 1967.

Table I. Characteristics of Mixed Finite Element Models Used in Numerical Studies

Model	Number of displacement nodes	Number of parameters per internal force (or Lagrange multiplier)	Number of quadrature points	Designation
One-dimensional	3	2	3	M3-2
	4	3	4	M4-3
Two-dimensional	9	4	9	M9-4

Table II. Minimum Frequencies Obtained by Two-Dimensional and Thin-Walled Beam (Converged) Models for the Cantilever Beam With Unsymmetric Channel Section (Fig. 2) and the Semicircular Beam With Unsymmetric Z-Section (Fig. 8)

Mode	Minimum frequencies for cantilever beam, Hz		Minimum frequencies for semicircular beam, Hz	
	Ω_{2d}	$\Omega_{converged}$	Ω_{2d}	$\Omega_{converged}$
1	11.64	11.66	12.14	12.48
2	19.64	19.67	23.12	23.08
3	40.94	41.09	44.14	42.71
4	58.52	58.97	50.90	50.88
5	103.6	103.9	92.71	91.42
6	113.9	114.6	100.2	92.71

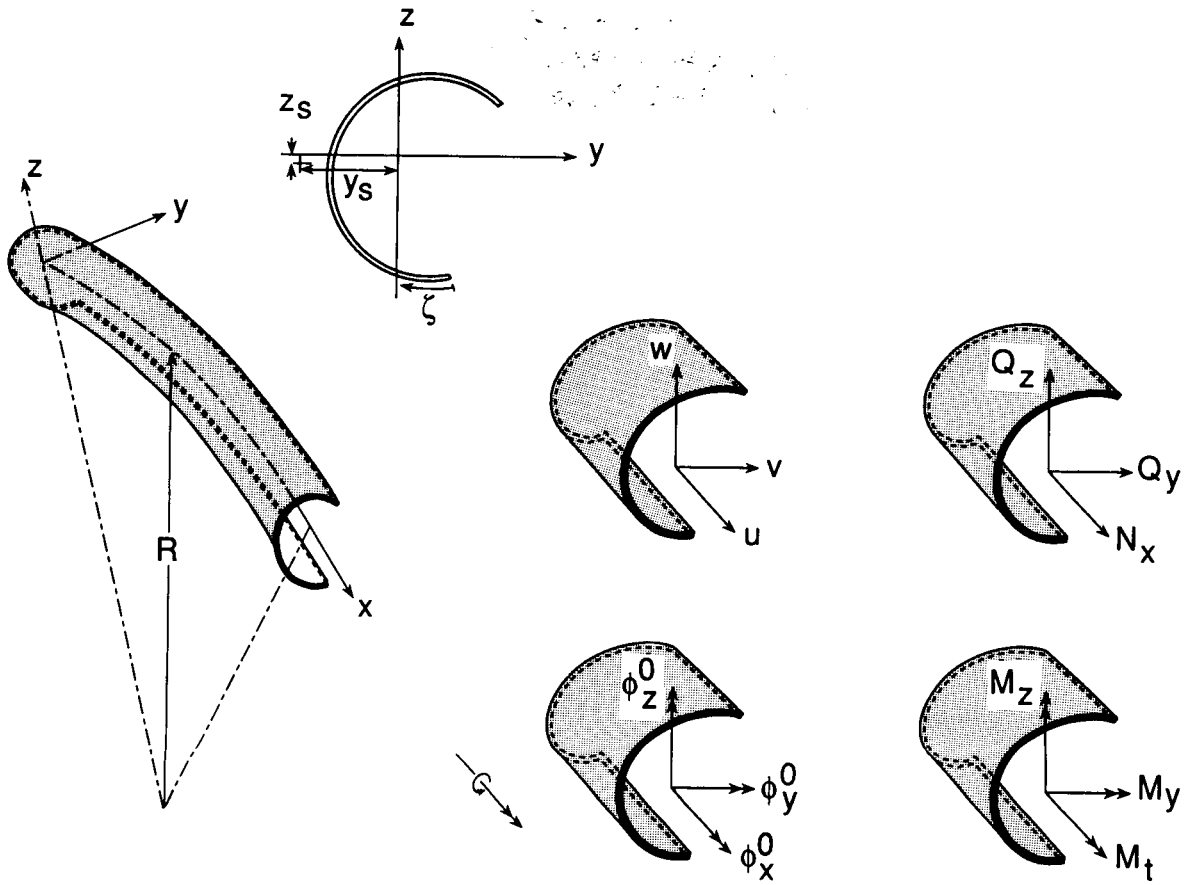

Figure 1. Characteristics of thin-walled beam and sign convention for internal forces and displacements.

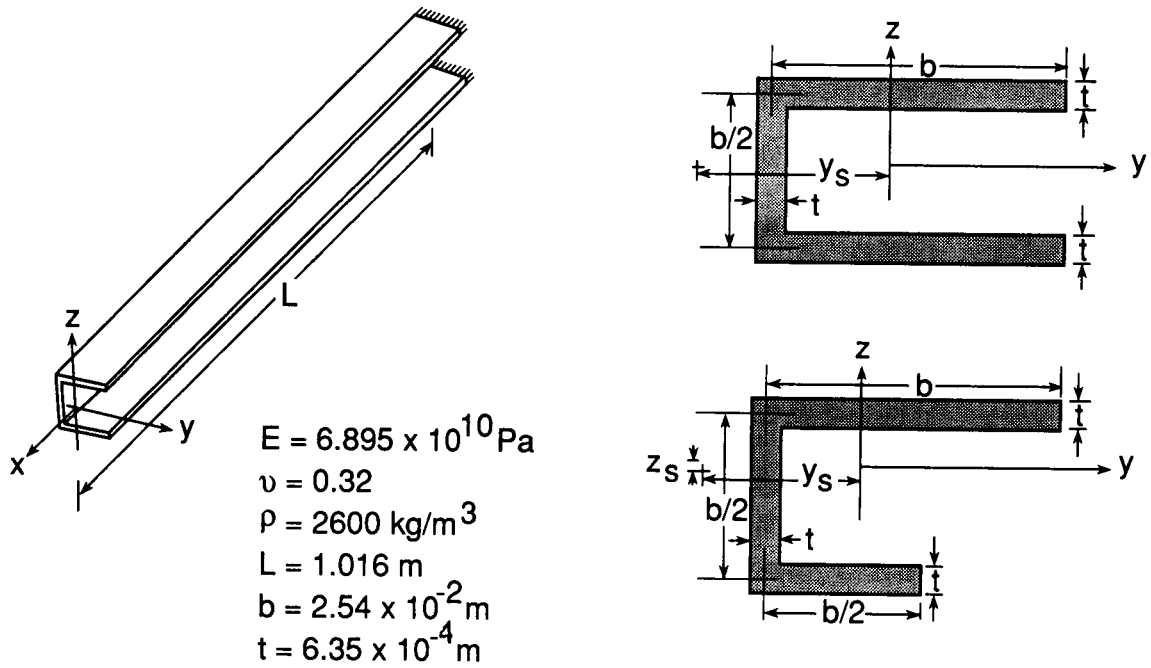

Figure 2. Cantilever beams with channel cross sections used in present study. The subscript s refers to shear center.

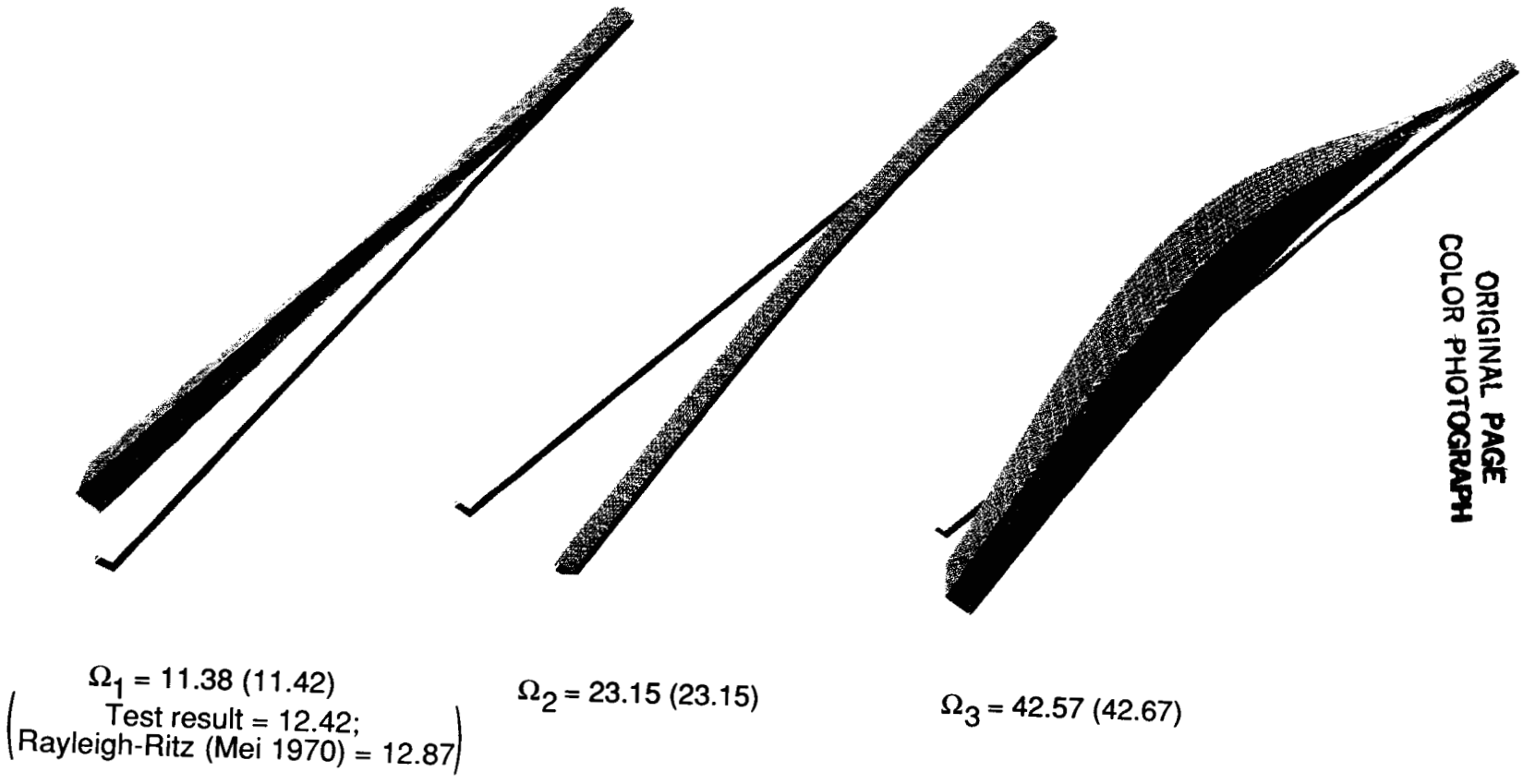

Figure 3. Vibration mode shapes for cantilever beam with symmetric channel section shown in figure 2. Numbers in parentheses are converged thin-walled beam frequencies (in hertz); other numbers are frequencies obtained by two-dimensional model.

ORIGINAL PAGE
COLOR PHOTOGRAPH

$\Omega_4 = 57.67\ (58.17)$ $\Omega_5 = 106.5\ (107.2)$ $\Omega_6 = 144.5\ (144.6)$

Figure 3. Concluded.

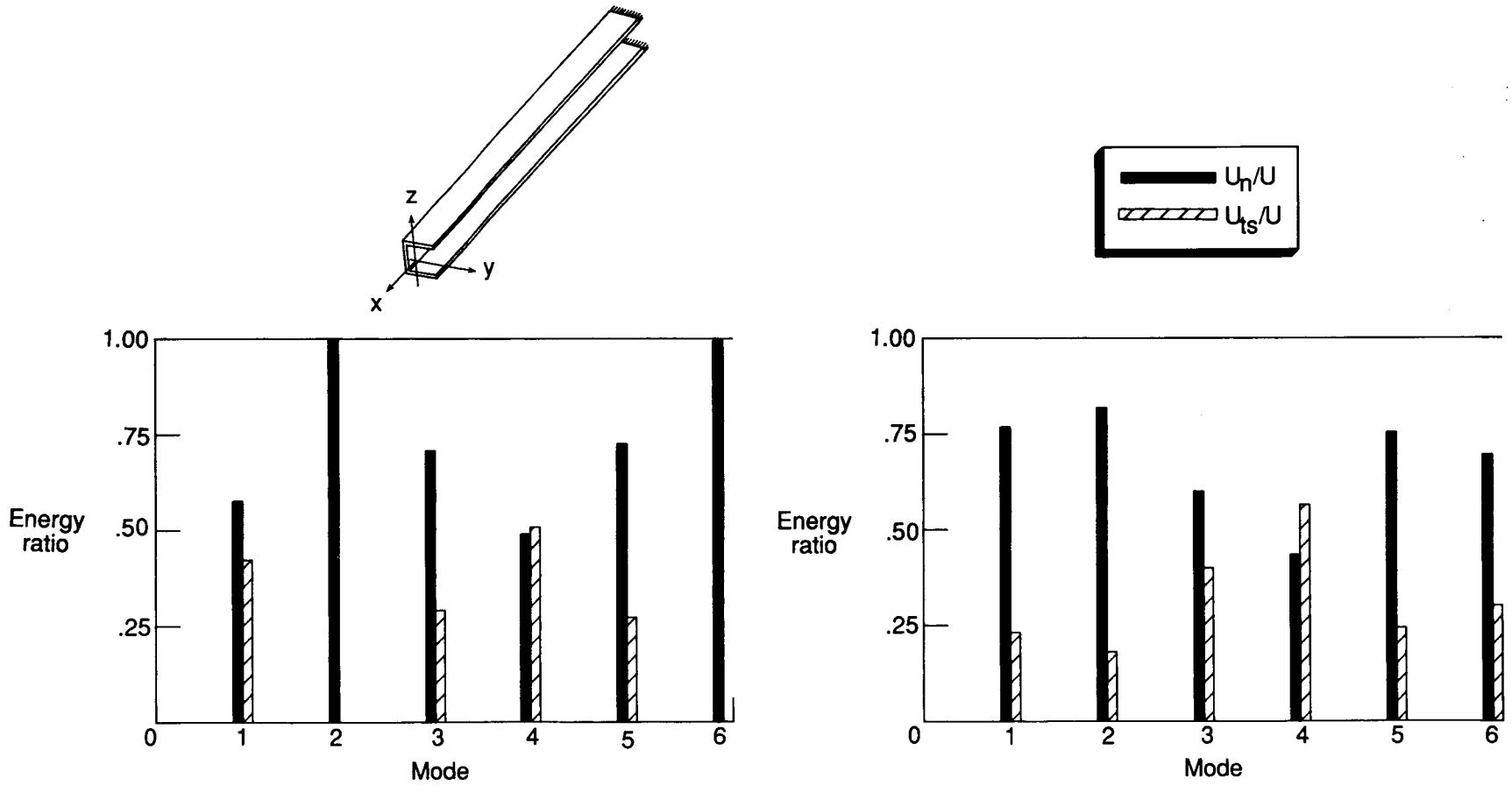

(a) Symmetric channel cross section.

(b) Unsymmetric channel cross section.

Figure 4. Strain energy ratios for different vibration modes of cantilever beam with channel cross section shown in figure 2. U_n is strain energy associated with N_x, M_y, M_z, and B_ω; and U_{ts} is strain energy associated with M_t.

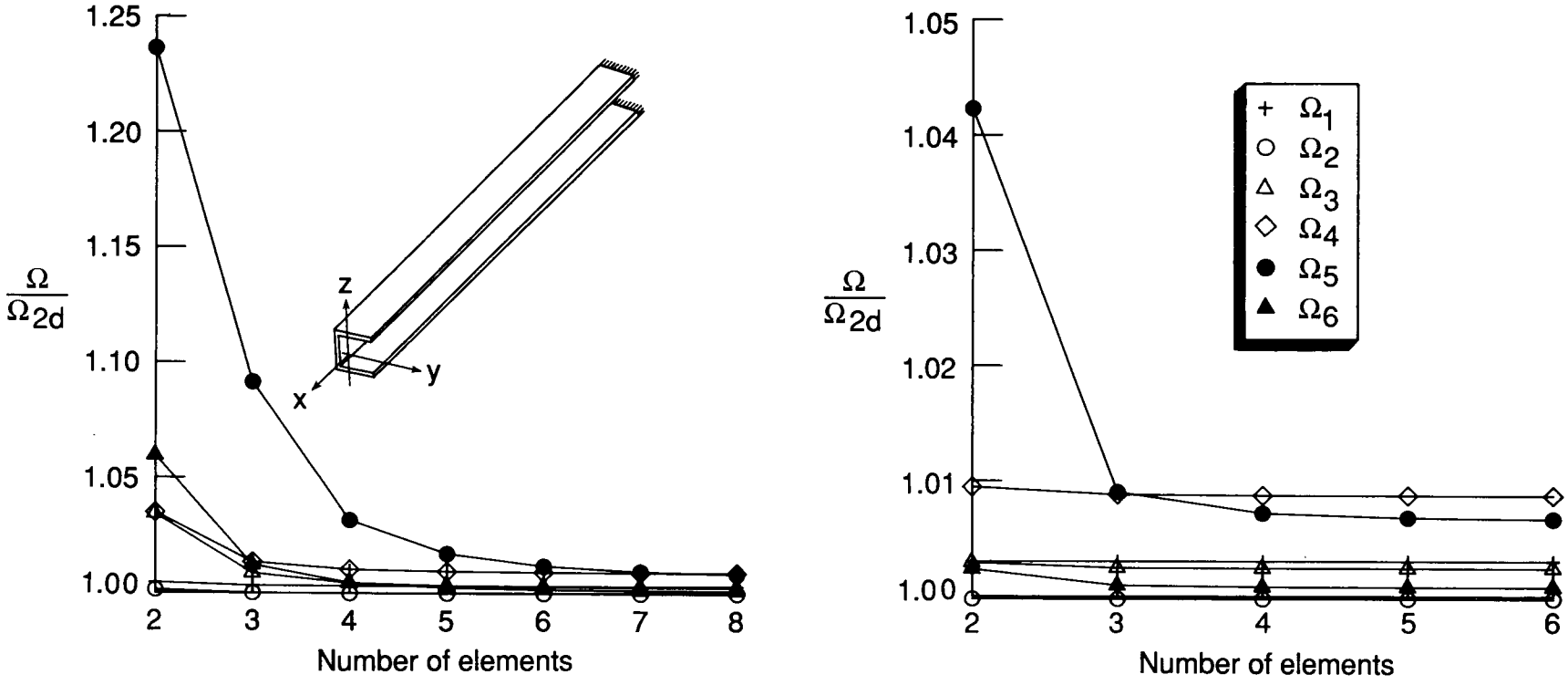

(a) M3-2 model.

(b) M4-3 model.

Figure 5. Accuracy and convergence of frequencies obtained by mixed models for cantilever beam with symmetric channel section shown in figure 2.

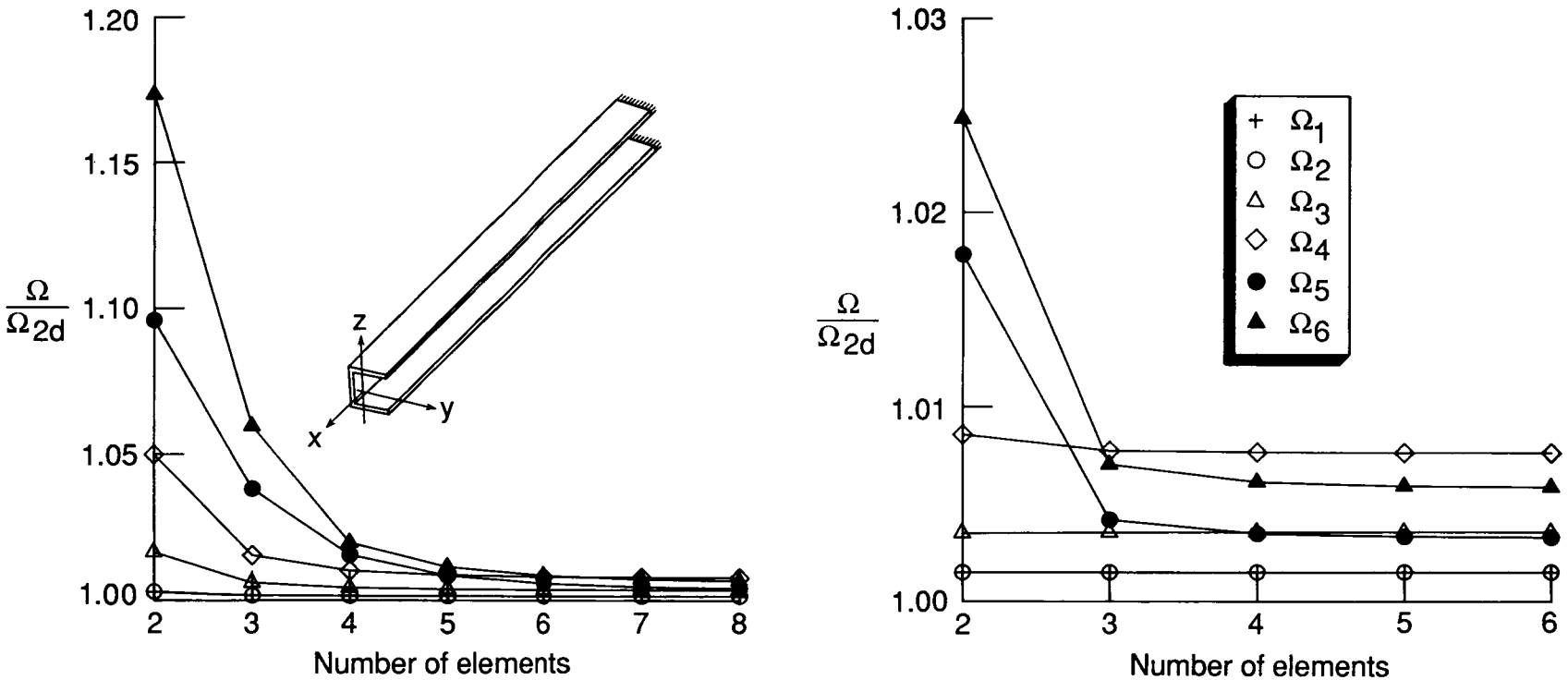

(a) M3-2 model.

(b) M4-3 model.

Figure 6. Accuracy and convergence of frequencies obtained by mixed models for cantilever beam with unsymmetric channel section shown in figure 2.

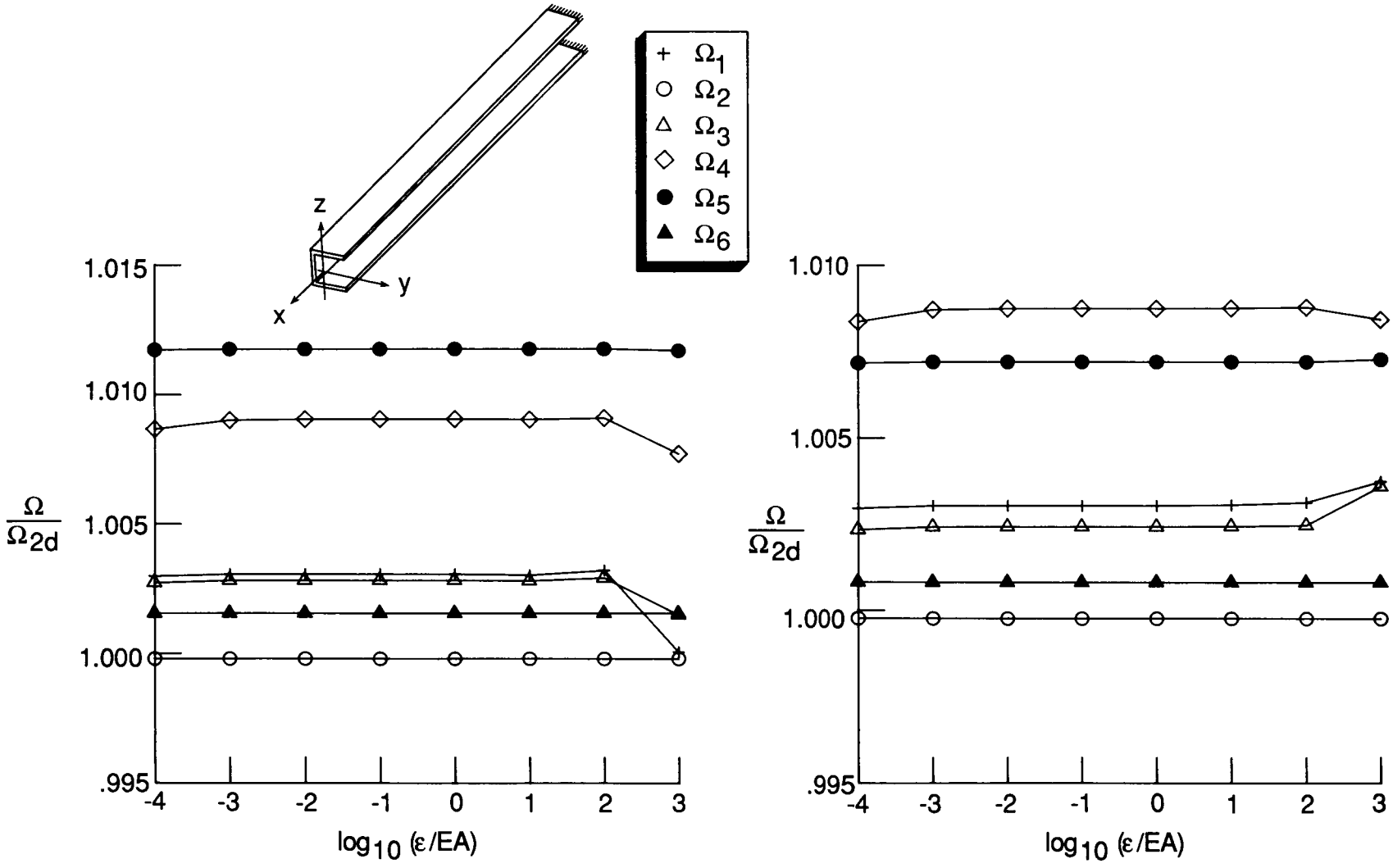

(a) Six elements with M3-2 model.

(b) Four elements with M4-3 model.

Figure 7. Effect of magnitude of penalty number on accuracy of vibration frequencies obtained by mixed models for cantilever beam with symmetric channel cross section shown in figure 2.

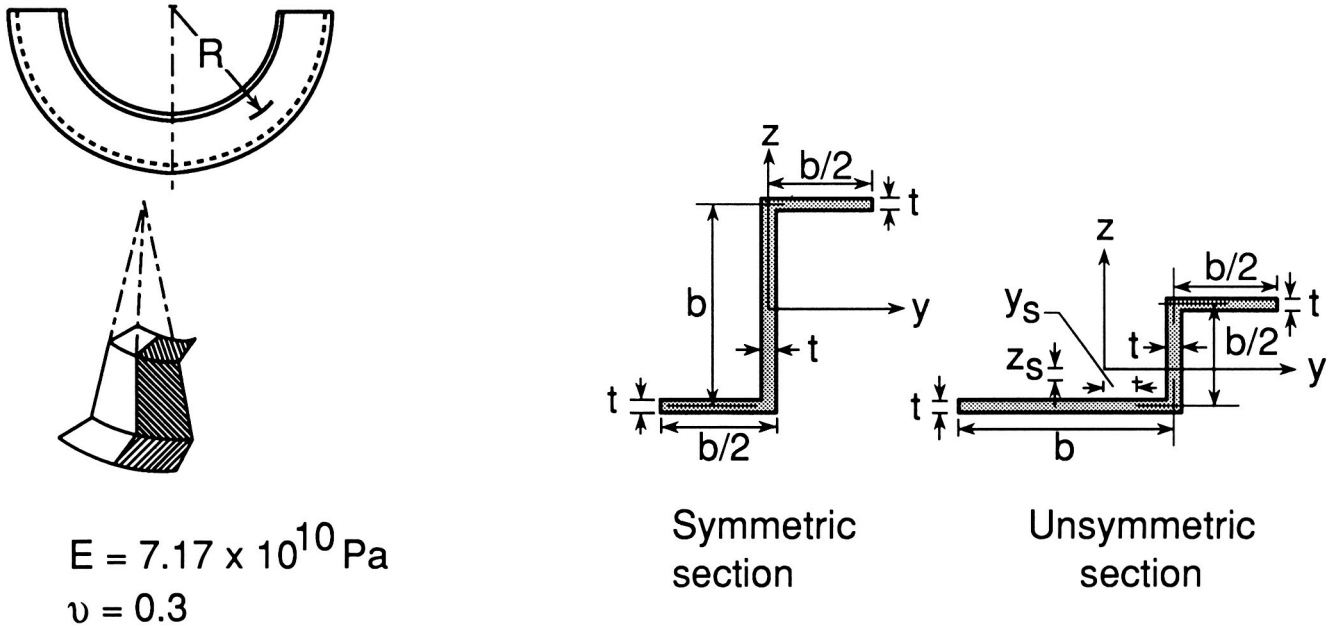

$E = 7.17 \times 10^{10}$ Pa

$\upsilon = 0.3$

$\rho = 2768$ kg/m^3

$R = 1.0$ m

$b = 5.08 \times 10^{-2}$m

$t = 6.0 \times 10^{-3}$m

Figure 8. Semicircular beams with Z-sections used in present study. The subscript s refers to shear center.

Ω_1 = 10.70 (11.10)

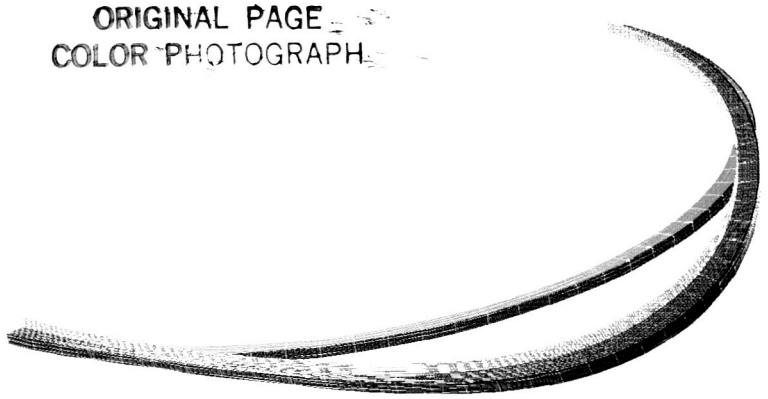

Ω_2 = 24.02 (24.17)

Ω_3 = 51.72 (52.13)

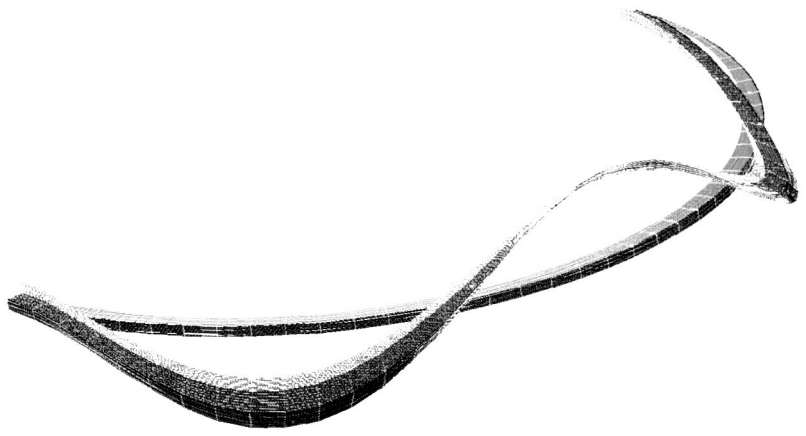

Figure 9. Vibration mode shapes for semicircular beam with symmetric Z-section shown in figure 8. Numbers in parentheses are converged thin-walled beam frequencies (in hertz); other numbers are frequencies obtained by two-dimensional model.

Ω_4 = 63.02 (64.41)

Ω_5 = 91.41 (92.12)

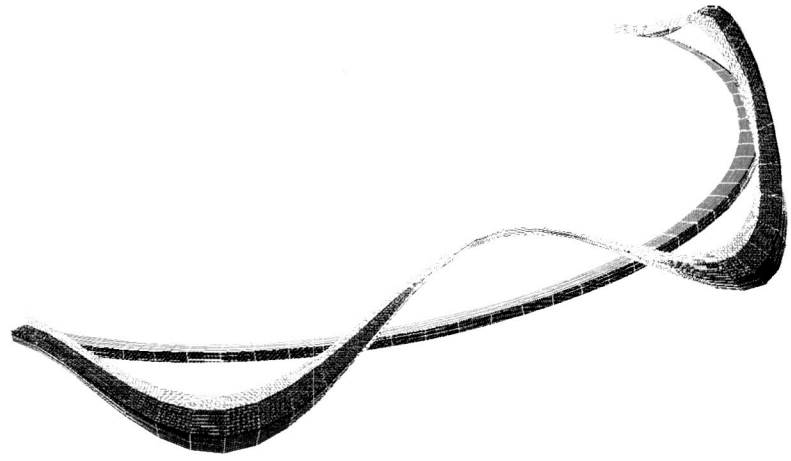

Ω_6 = 128.7 (131.5)

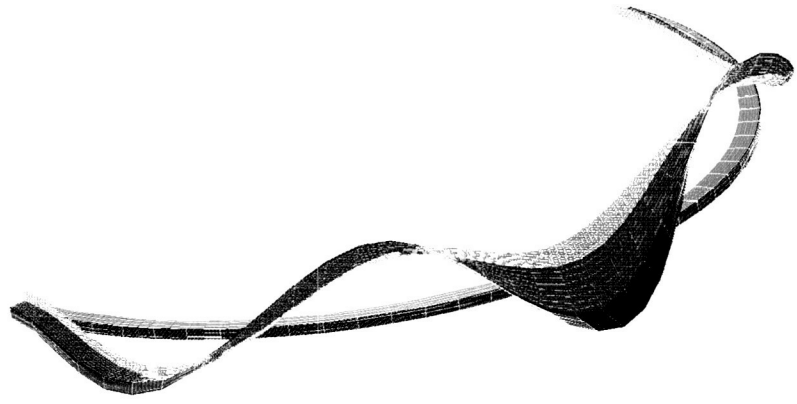

Figure 9. Concluded.

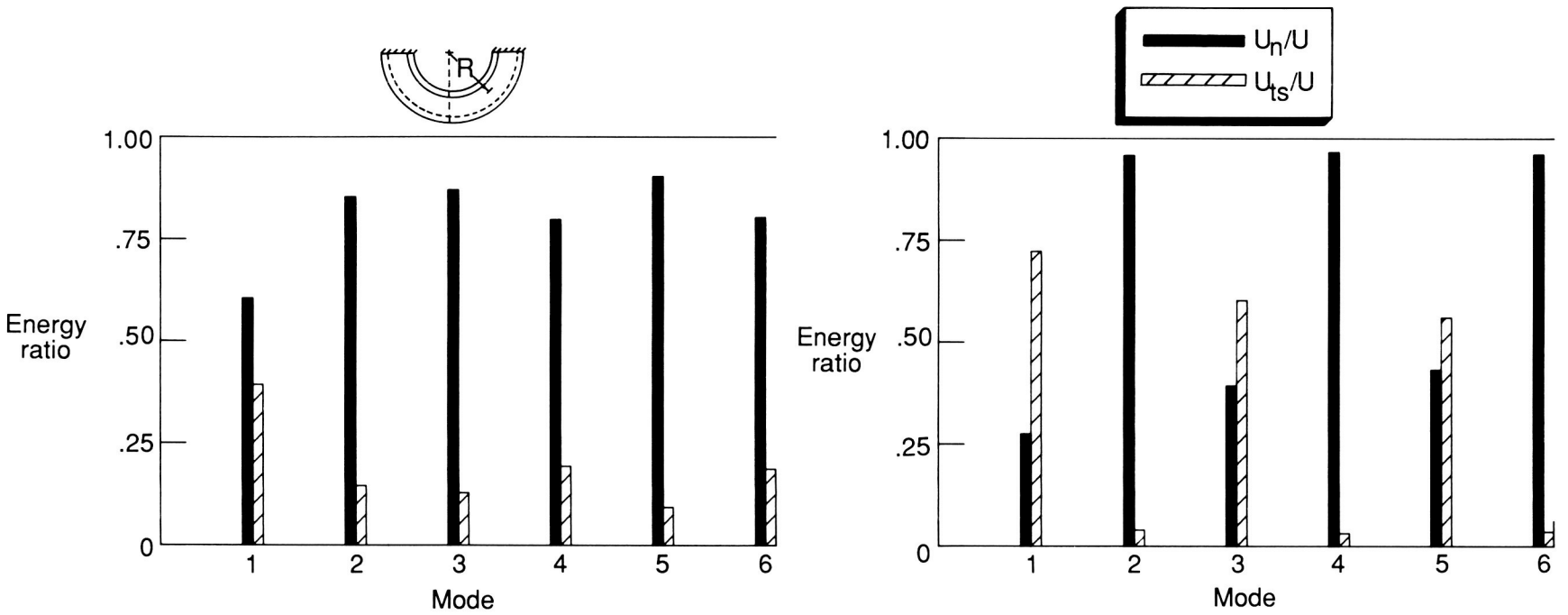

(a) Symmetric Z-section.

(b) Unsymmetric Z-section.

Figure 10. Strain energy ratios for different vibration modes of semicircular beam with Z-sections shown in figure 8. U_n is strain energy associated with N_x, M_y, M_z, and B_ω; and U_{ts} is strain energy associated with M_t.

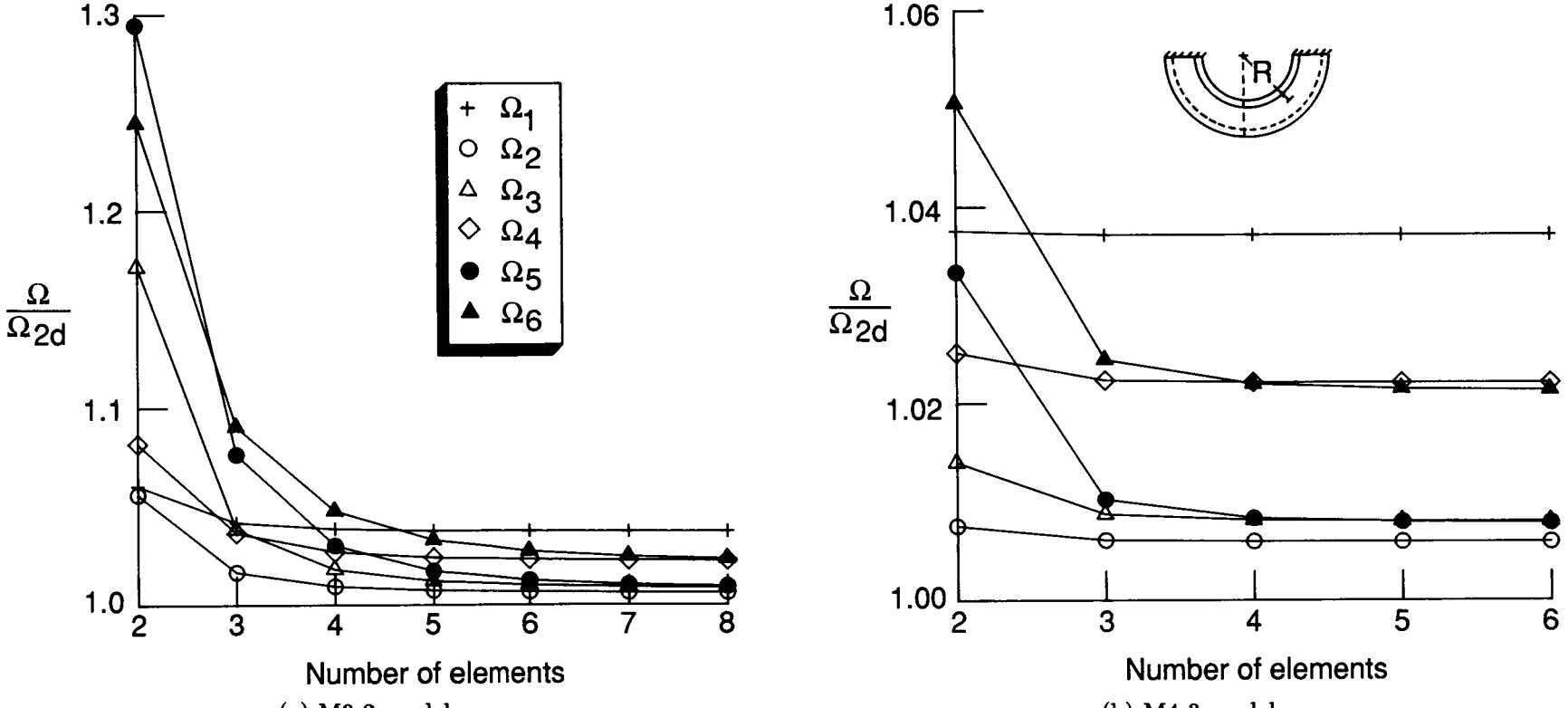

(a) M3-2 model.

(b) M4-3 model.

Figure 11. Accuracy and convergence of frequencies obtained by mixed models for semicircular beam with symmetric Z-section shown in figure 8.

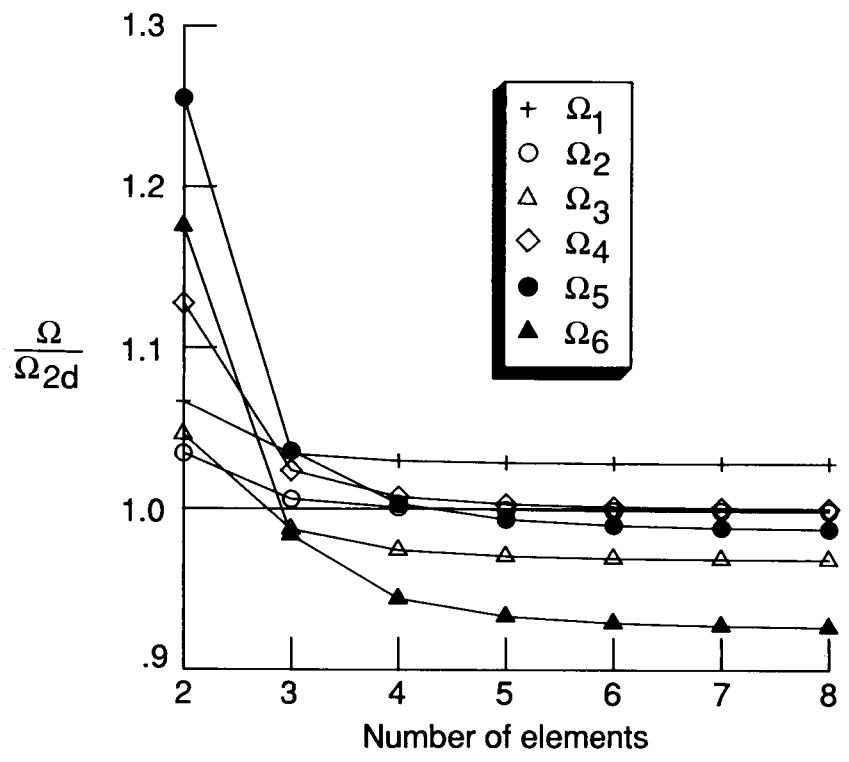

(a) M3-2 model.

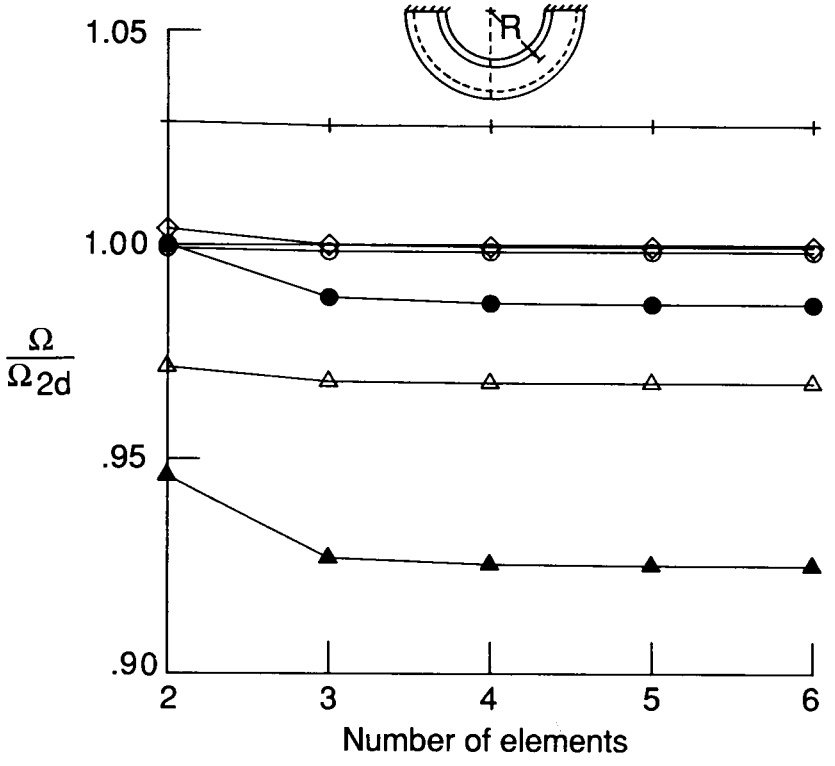

(b) M4-3 model.

Figure 12. Accuracy and convergence of frequencies obtained by mixed models for semicircular beam with unsymmetric Z-section shown in figure 8.

NASA
National Aeronautics and Space Administration

Report Documentation Page

1. Report No.	2. Government Accession No.	3. Recipient's Catalog No.
NASA TP-2868		

4. Title and Subtitle	5. Report Date
Mixed Finite Element Models for Free Vibrations of Thin-Walled Beams	February 1989
	6. Performing Organization Code
7. Author(s)	8. Performing Organization Report No.
Ahmed K. Noor, Jeanne M. Peters, and Byung-Jin Min	L-16506
9. Performing Organization Name and Address	10. Work Unit No.
NASA Langley Research Center Hampton, VA 23665-5225	505-63-41-02
	11. Contract or Grant No.
12. Sponsoring Agency Name and Address	13. Type of Report and Period Covered
National Aeronautics and Space Administration Washington, DC 20546-0001	Technical Paper
	14. Sponsoring Agency Code

15. Supplementary Notes

Ahmed K. Noor, Jeanne M. Peters, and Byung-Jin Min: The George Washington University, Joint Institute for Advancement of Flight Sciences, Langley Research Center, Hampton, Virginia.

16. Abstract

Simple, mixed finite element models are developed for the free-vibration analysis of curved, thin-walled beams with arbitrary open cross section. The analytical formulation is based on a linear, Vlasov-type, thin-walled beam theory with the effects of flexural-torsional coupling, transverse shear deformation, and rotary inertia included. The fundamental unknowns consist of seven internal forces and seven generalized displacements of the beam. The element characteristic arrays are obtained by using a modified form of the Hellinger-Reissner mixed variational principle. Only C^0 continuity is required for the generalized displacements. The internal forces and the Lagrange multiplier are allowed to be discontinuous at interelement boundaries. Numerical results are presented to demonstrate the high accuracy and effectiveness of the elements developed. The standard of comparison is taken to be the solutions obtained by using two-dimensional plate/shell models for the beams.

17. Key Words (Suggested by Authors(s))	18. Distribution Statement
Thin-walled beams Perturbed Lagrangian formulation Flexural-torsional coupling Free vibrations Mixed finite element models	Unclassified—Unlimited Subject Category 39

19. Security Classif.(of this report)	20. Security Classif.(of this page)	21. No. of Pages	22. Price
Unclassified	Unclassified	27	A03

NASA FORM 1626 OCT 86 NASA-Langley, 1989

For sale by the National Technical Information Service, Springfield, Virginia 22161-2171